Max-Planck-Institut für Meteorologie

REPORT No. 27

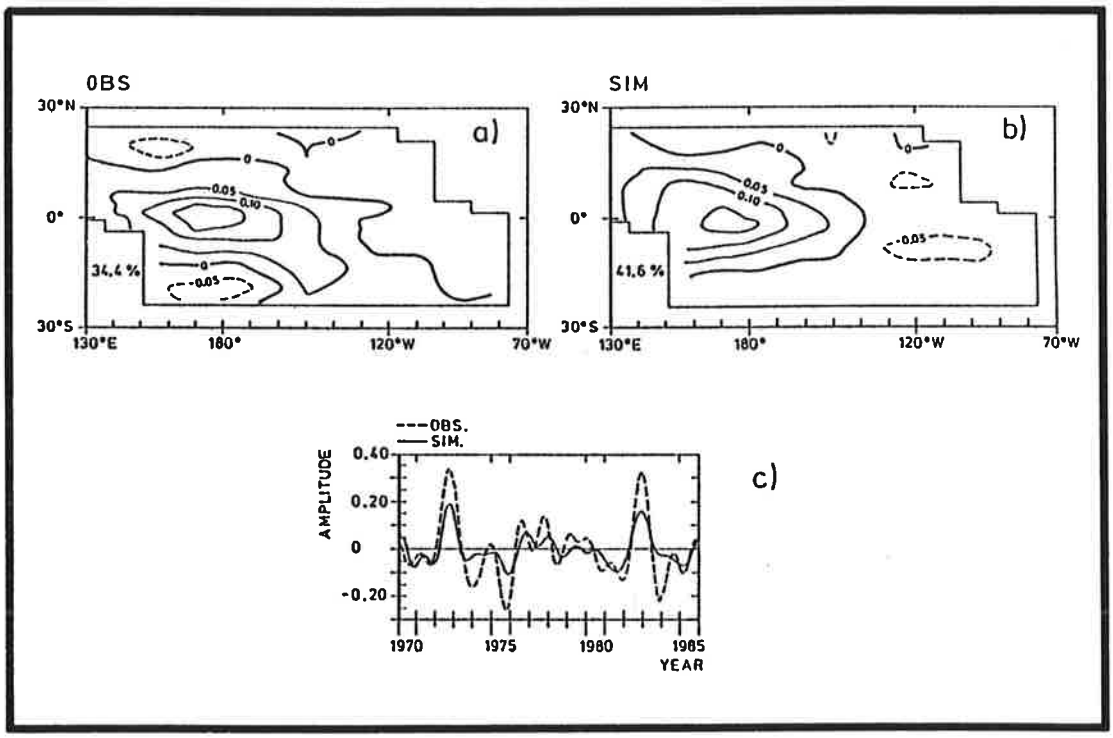

ANALYSES OF TROPICAL ANOMALIES SIMULATED BY AN AGCM

by

MOJIB LATIF • JOACHIM BIERCAMP • HANS VON STORCH
MICHAEL McPHADEN • EDILBERT KIRK

HAMBURG, APRIL 1989

AUTHORS:

MOJIB LATIF
MAX-PLANCK-INSTITUT
FUER METEOROLOGIE

JOACHIM BIERCAMP
MAX-PLANCK-INSTITUT
FUER METEOROLOGIE

HANS VON STORCH
MAX-PLANCK-INSTITUT
FUER METEOROLOGIE

MICHAEL McPHADEN
PACIFIC MARINE
ENVIRONMENTAL LABORATORY
SEATTLE
WASHINGTON
USA

EDILBERT KIRK
METEOROLOGISCHES INSTITUT
DER UNIVERSITAET HAMBURG
BUNDESSTRASSE 55
D-2000 HAMBURG 13
F. R. GERMANY

MAX-PLANCK-INSTITUT
FUER METEOROLOGIE
BUNDESSTRASSE 55
D-2000 HAMBURG 13
F.R. GERMANY

Tel.: (040) 4 11 73-0
Telex: 211092
Telemail: MPI.Meteorology
Telefax: (040) 4 11 73-298

Analyses of Tropical Anomalies Simulated by an AGCM

Mojib Latif, Joachim Biercamp, Hans von Storch
Max-Planck-Institut für Meteorologie, Hamburg, FRG

Michael McPhaden
Pacific Marine Environmental Laboratory, Seattle, Washington, USA

Edilbert Kirk
Meteorologisches Institut der Universität Hamburg, FRG

ABSTRACT

The ECMWF-T21 atmospheric GCM was forced with observed near-global SST from January 1970 to December 1985. Its response over the Pacific Ocean is compared with various observations: Tahiti and Darwin station sea level pressure, equatorial buoy and COADS surface wind observations, FSU wind stress analyses and NMC analyses of 850 mb zonal wind and of outgoing longwave radiation.

The time dependent SST clearly induces a Southern Oscillation in the model run which is apparent in the time series of all considered variables. The phase of the AGCM Southern Oscillation is as observed but its low frequency variance is too weak and is mainly confined to the Western Pacific. The model is successful in reproducing the warm events of 1972/73 and 1982/83 and the cold event 1970/71, but it shows only weak indications of the cold events 1973/74 and 1975/76 and the warm event 1976/77.

Because of the GCM's use as the atmospheric component in a coupled TOGA model the response of an equatorial oceanic primitive equation model to both, the modeled and observed wind stress is examined. The ocean model responds to the full observed wind stress forcing almost identically as to the forcing described by the first two low-frequency EOFs of the observations only. These first two EOFs describe a regular eastward propagation of the SO signal from the Western Pacific to the Central Pacific within about a year. The ocean model's response to the modeled wind stress is too weak and similar to the response to the observed forcing if truncated to the first EOF only. That is, the observed SO appears as a sequence of propagating patterns but the simulated SO as a standing oscillation.

The nature of the deviation of simulated wind stress from observations is further analyzed by means of Model Output Statistics (MOS). It is shown that the MOS-corrected simulated wind stress, if used as forcing for the OGCM, leads to a significant enhancement of low frequency SST variance, which is most pronounced in the Western Pacific.

1. Introduction

In this paper we consider our AGCM's ability to reproduce observed tropical low frequency anomalies. The background for doing so is that the model, which is the T21 version of the ECMWF GCM, is used as the atmospheric component in a coupled GCM of the Tropical Pacific Ocean and the Global Atmosphere (TOGA). The oceanic component is simulated with the oceanic GCM described by Latif (1987). The coupled GCM has been used to study the effect of strong westerly wind bursts over the Western Pacific (Latif et al., 1988a). In an other experiment we found the coupled GCM unable to generate self-excited low-frequency variability (Latif et al., 1988b). The reasons for the model's failure were not quite clear and we speculated that the atmospheric component might be blamed for part of the failure.

GCM data are also used to improve operational wind field analyses by blending observed winds with nowcasted winds (Leetma and Ji, 1988). Consequently, it is of interest to compare the T21 simulated winds and other parameters with observations, and to examine the sensitivity of the ocean circulation to deviations between these data sets.

Recently a multi year simulation was performed with the ECMWF atmospheric GCM in its T21 resolution using observed SST changes during the period January 1970 to December 1985 to force the model. Here we investigate the tropical response of the T21 model to these time dependent SST anomalies, which include several cold and warm events, and compare the model data with observations that were available to us.

Similar experiments have been conducted at different institutions so far: Lau (1985) performed two 15-year integrations with the atmospheric GCM developed at the Geophysical Fluid Dynamics Laboratory (GFDL), using observed month-to-month SST during the period 1962 to 1976 as lower boundary condition over the Tropical Pacific. He shows that the model's circulation in the tropics responds in a realistic way to SST changes during El Niño events. Graham et al. (1988) report on the response of the National Center for Atmospheric Research GCM to prescribed SST anomalies for the period 1961 to 1972 in terms of tropical Pacific wind stress (this run was performed by Chervin, 1986): They find that the spatial configuration of the simulated wind stress resembles the observed one, but there is less agreement in the non-equatorial regions and the amplitude of the model response is too weak.

In this contribution we verify the simulated data quantitatively by comparing them to observational data of various sources. These data are described in detail in Section 2.

In Section 3 we compare time series of simulated surface wind at some equatorial positions with data observed at equatorial buoys. These in situ measurements are regarded as being trustworthy, but the time series of wind components are only available at a few locations and are rather short (a few years) with respect to the typical ENSO time scale of two and more years.

In Section 4 we consider the Southern Oscillation Index and long time series extracted from large scale analyses of tropospheric equatorial wind, outgoing longwave radiation (used as indicator for precipitation) and surface wind stress. In the latter data which are not directly observed but are analyzed using information of limited accuracy and spatial extent we are less confident. With respect to the atmosphere-ocean coupling, however, it is the large scale response rather then the local one we are interested in.

After having found systematic differences between the simulated and the observed surface wind field, we deal in Section 5 with the sensitivity of an ocean GCM to these systematic errors in the wind field. For this purpose a Tropical Pacific Ocean primitive equation model has been integrated using the observed wind stress and the simulated wind stress as forcing.

In Section 6 we test the "Model Output Statistic" (MOS) approach, known from Numerical Weather Predictions, whether it is successful in overcoming practically the afore mentioned systematic errors.

The paper is finished with a discussion of the results in the final Section 7.

2. DATA

2.1 Model Data

The model data were obtained from a 16 year integration with the T21 version of the AGCM of the ECMWF (Fischer, 1987; Storch, 1988). The SST has been specified according to CAC analysis of 40°S-60°N (January 1970 to December 1980) and global (January 1981 to December 1985) SST (Reynolds, 1988). Over land temperature and moisture have been calculated prognostically using prescribed deep soil temperature and moisture. The distribution and surface temperature of sea and land ice have been prescribed. The initial conditions are taken from January 1, year 2 of a control run with climatological SST. The model output is stored as monthly means, which are indexed by the date of the SST anomaly. We use surface wind stress, 10m wind, 850 mb wind and rainfall.

2.2 Verification Data

Besides the sea level pressure difference between the stations at Darwin and Tahiti, defining the well known Southern Oscillation Index (SOI), we use wind, pseudostress and outgoing longwave radiation (OLR) from different origins:

(A) Surface wind (buoy data)

In situ observations from equatorial buoys (McPhaden and Taft, 1988) at 110°W (March 80; Aug. 80 - Dec. 82; Nov. 83 - Nov. 84; May 85 - December 85), at 124°W (Nov. 83 - Oct. 84, May 85 - Sep. 85) and 140°W (May 84 - July 85, Oct. 85 - Dec. 85). The measurements were done at a level of 3.8 m. Assuming neutral stability, which is reasonable over the cold Eastern Pacific surface water, we approximate the 10 m wind by multiplying the measurements by the factor of 1.1 (Large and Pond, 1981).

It should be noted that the monthly buoy wind data are based on two types of vector average measurements. Most are made from a cup and vane anemometer (15 minute averaging interval) and some are made from a propeller and vane anemometer (2 hour averages). Individual two hour averages in the zonal and in the meridional component determined from these instruments are consistent with one another to within 0.5 m/s based on a 4 months experiment on the equator at 140°W (Freitag et al., 1988). The mean differences were 0.09 m/s in the zonal

component (propeller larger) and 0.15 m/s in the meridional component (cup larger).

(B) Surface wind (analyses)

Monthly mean 10 m wind components on a $2^{\circ}x2^{\circ}$ grid for the period 1950 to 1979 are available from COADS (Comprehensive Ocean-Atmosphere Data Set; for references see Wright, 1988). COADS is based largely on ship observations and only little spatial and temporal averaging has entered the final data set. Along the equator the data are very sparse, but we believe that sufficient data is available to estimate the mean annual cycles shown in Figure 1.

For 1980 to 1986, COADS "interim" data became available recently. Having only a few entries on the equator, it is not useful to consider monthly anomalies on the $2^{\circ}x2^{\circ}$ grid as was done with the long term monthly means. Instead the numbers plotted in Figures 2, 3 and 4 are area means on a 4° (latitude) and 10° (longitude) grid. It may be anticipated that one should not be very confident in these anomalies, as the entries are sparse, coming from areas with strong horizontal gradients and being in part subjective.

(C) 850 mb zonal wind and precipitation

Precipitation is derived from OLR using the simple Arkin (1982)-relationship for anomalies, i.e., precipitation [mm/day] = -OLR [W/m^2] / 5.7. NMC (National Meteorological Center (USA)) analyses of equatorial 850 mb zonal wind covering the time period May 1974 to February 1985 and of OLR from May 1974 to March 1978 and from January 1980 to February 1985 are available (Arkin, 1982; Trenberth and Olsen, 1988). Note that the wind data are not really "observed" but the output of the NMC operational forecast model.

(D) Pseudo wind stress

FSU (Florida State University) analyses of pseudo wind stress fields (Goldenberg and O'Brien, 1981; and Legler and O'Brien, 1984). These fields have been obtained from subjective analyses of ship wind observations over the Tropical Pacific. The data set consists of monthly mean pseudo stresses for the period 1961 to 1985. The resolution is $2^{\circ}x2^{\circ}$, the analyzed area extends from $29^{\circ}N$ to $29^{\circ}S$ and from $124^{\circ}E$ to $70^{\circ}W$. As described by Goldenberg and O'Brien (1981) there was poor data coverage on and south of the equator so that the analyses is of limited reliability in these data sparse regions. To

obtain wind stress the data were multiplied by ρc_d, where ρ = 1.2 kg/m^3 is the density of air and $c_d = 1.5 \cdot 10^{-3}$ the drag coefficient.

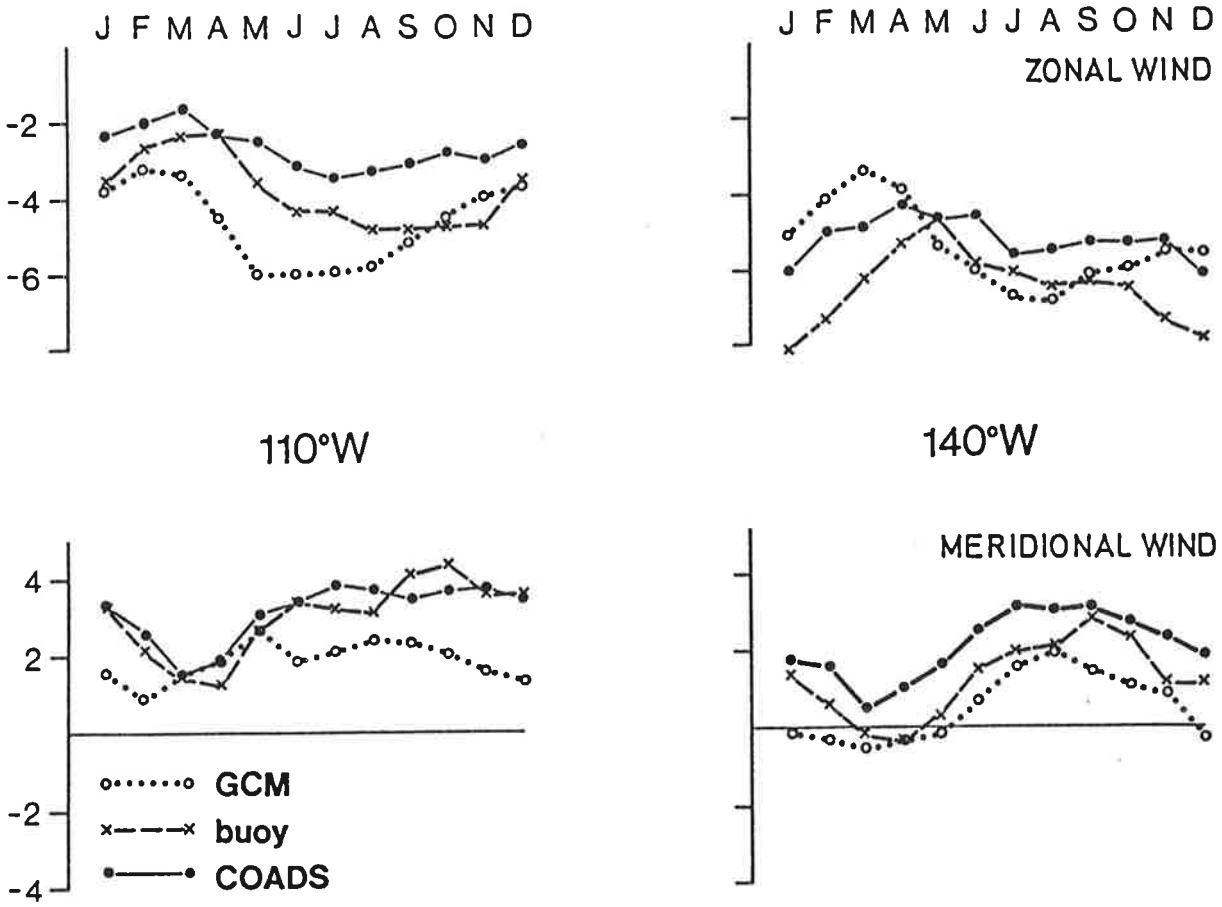

Figure 1: Mean annual cycles of zonal (top row) and meridional (bottom row) 10 m wind at 110°W (left column) and at 140°W (right column). Units: m/s. Crosses line: buoy data; the raw data was taken at 4 m, from which an estimate of the 10m wind was obtained by multiplication by 1.1. Solid circles: calculated from January 1950 - December 1979 COADS. Open circles: GCM data: a time-area mean from 2.8°S - 2.8°N and January 1970 to December 1985 is shown.

3. Results: Local Surface Wind Response

In this section we compare the simulated surface winds at three locations on the equator (110°W, 124°W and 140°W) to in situ observations from equatorial buoys (data set A). As an additional reference COADS (data set B) is used.

It should be noted that the GCM winds shown in this section represent area averages over a grid box of 5.6° × 5.6°, because there is no grid point located directly on the equator. Therefore, there may arise some problems in defining a "local" response and the verification of the GCM winds may suffer from the low resolution.

3.1 Annual Cycle

At 124°W there are too few buoy data to define a mean annual cycle, but at 110°W and 140°W there are sufficient buoy data available to do so (in two months only 2 samples, otherwise at least 3 samples per calendar month). The observed and simulated annual cycles of the zonal and meridional wind component at these two locations are shown in Figure 1: The COADS annual cycle has been composed from data from 1950-79 (thus being independent from the buoy data annual cycle) and the GCM annual cycle from the 16 year run.

The COADS and buoy data annual cycles show qualitative resemblance but quite large quantitative deviations from each other: Maximum deviations are of the order of 2 m/s (40%), which is likely due to insufficient sampling of the buoy data annual cycle and to insufficient accuracy and sampling frequency of the COADS entries. The buoy zonal winds are mostly stronger than the COADS zonal winds. The buoy meridional winds at 140°W are weaker than in COADS, and in March and April northerly winds are reported from the buoys, while the COADS winds remain southerly. Note, however, that the buoy data estimate is based on two samples only: March and April 1985 and 1986.

The simulated data are of the same order of magnitude as the buoy data, but tend to be somewhat weaker. An exception is the zonal wind at 110°W. Here the model simulates during February to October stronger than observed winds at the buoys. Maximum deviations are of the order of 3 m/s, which is quite substantial. The annual cycles are similar, but the simulated cycles have

minima in February/March, which is one or two months prior to the buoy data annual cycle's minima in March/April/May.

Comparing the present findings with an earlier evaluation (Biercamp and Storch, 1987) of the GCM's wind stress using Han and Lee's (1981) wind stress climatology, we find at 110°W an apparent contradiction: the zonal Han and Lee wind stress is about twice the simulated value but the zonal GCM wind is in most months larger than the buoy winds. This can be related to two facts, the first being that the meridional wind enters the calculation of the zonal wind stress. At 110°W the model underestimates the meridional wind heavily, which in turn might be related to the model's inability to reproduce an ITCZ of sufficient strength (Kiladis, 1988). The second point, that may contribute to the bias in quality between the monthly means of simulated stress and of surface wind is the fact that the monthly mean of wind stress is made up from two components, the effect of the mean flow and the effect of transient features. The latter is too weakly simulated because the model apparently underestimates the high frequency variability in the Eastern Tropical Pacific.

3.2 Anomalies

The deviations from the annual cycle for the GCM, the buoy and COADS at 110°W and at 140°W are shown in Figures 2 and 3. The month-to-month variations may be attributed mainly to the tropical 30-60 day wave which state is not controlled by SST variations. It is therefore reasonable that the modeled and observed data vary incoherently on time scales up to a few months.

The COADS zonal wind anomalies at 140°W (Fig. 3) exhibit much more high frequency variance than the buoy data which is probably related to the particularly poor ship wind data density at this location. In spring 1985 the COADS zonal wind anomalies seem to be systematically larger (1-3 m/s) than the buoy data, while in fall 1985 easterly wind anomalies prevailed according to COADS and the buoy data indicated normal conditions at that location. In case of the 110°W zonal wind anomalies (Fig. 2) a strange pattern of similarity and dissimilarity between the buoy data anomalies and the COADS anomalies appears: Until February 1982 the zonal wind anomalies curves are well correlated, but this is no longer true for anomalies thereafter. Before February 1982 the mean differences are of the order of 0.5 m/s, and the anomalies are very close to each other in most cases. After February 1982 typical differences are of the order of 2 m/s, and the signs of the anomalies are mostly different. In

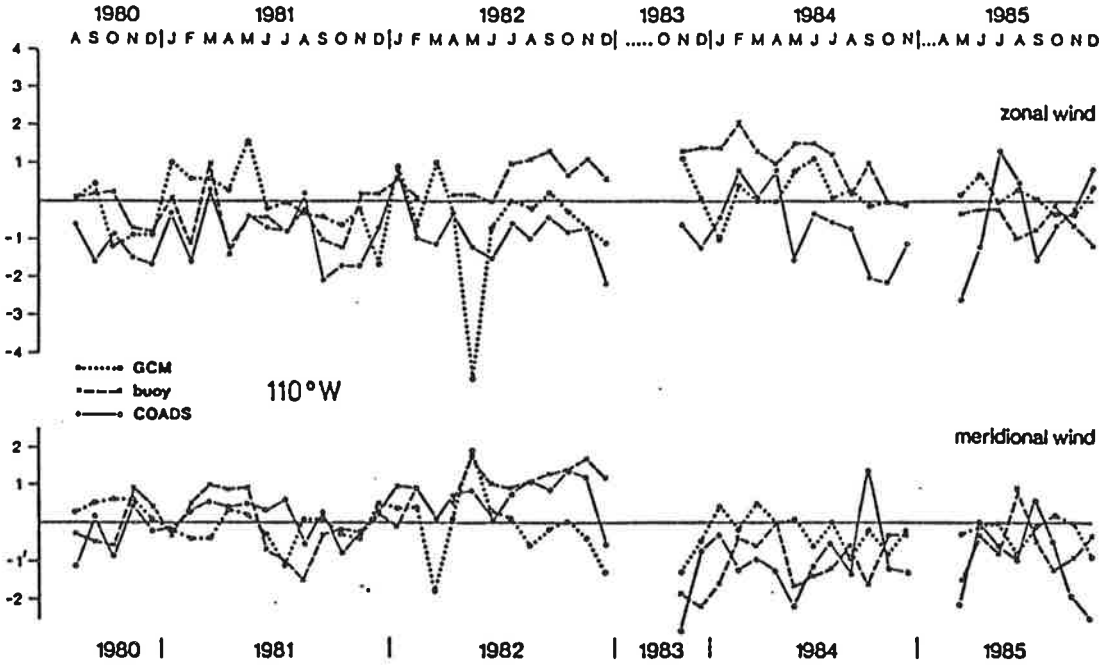

Figure 2: Time series of anomalous zonal (top) and meridional (bottom) 10 m wind at 110°W as reported from the buoy (crosses) and as simulated by the GCM (open circles). The COADS anomalies taken from a 4°x10° latitude-longitude grid are added (filled circles). Units: m/s.

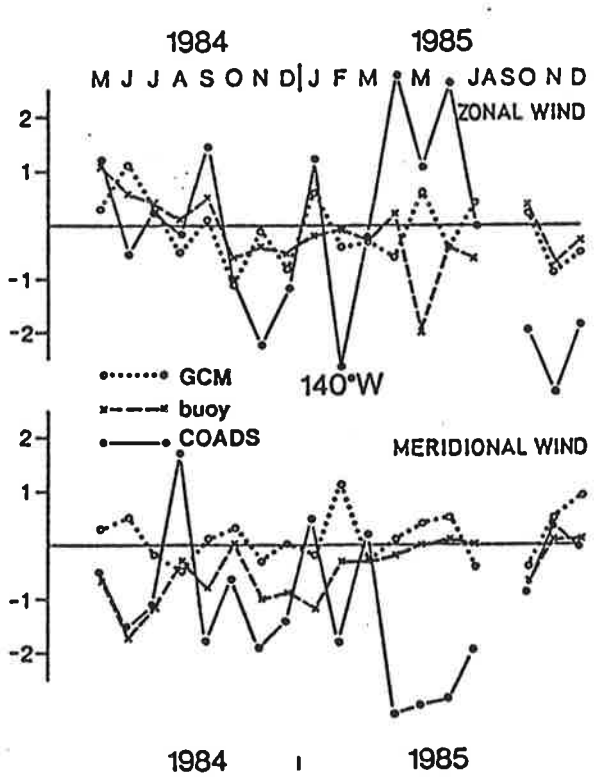

Figure 3: As Figure 2, but at 140°W.

particular, it may be inferred from the buoy data that during the El Niño event 1982/83 there have been westerly wind anomalies at 110°W during the entire event, while the COADS data reveal easterly zonal wind anomalies until the end of 1982. If, however, the COADS anomalies were calculated using the 1980-86 mean instead of the 1950-79 mean (not shown), the buoy and the ship data curves are in much better agreement: In September 1982, for example, COADS reveals anomalies of -0.4 m/s and 1.1 m/s, if the 1950-79 and 1980-86 mean is used, respectively. The latter number compares favorably with the 1.3 m/s derived from the buoy observations. The FSU data (data set D), however, indicate easterly zonal stress anomalies for almost the entire year 1982 and positive anomalies mostly during 1983.

The meridional wind anomalies given by the two observed data sets are quite similar apart from a significant deviation from April to July 1985 at 140°W (Fig. 3).

The comparison of the buoy data anomalies and the GCM anomalies leads to the following results: At both considered positions, 110°W (Fig. 2) and 140°W (Fig. 3), the GCM data are more noisy than the buoy data. There is only limited correspondence between buoy data anomalies and GCM anomalies. On the month-to-month time scale, no similarity exists. On longer time scales there is some coincidence at least with respect to the general shape of the curves. The model is more successful in simulating the wind anomalies at 140°W than at 110°W.

The model fails to reproduce the anomalies observed during the El Niño event of 1982/83: According to the buoy data, this event is accompanied with westerly and northerly wind anomalies of more than 1 m/s, but in the GCM no persistent anomalies exist.

At 124°W, an annual cycle cannot be derived from the buoy data. Therefore, absolute values are shown in Figure 4. For comparison, the mean annual cycles as derived from the 1950-79 COADS are added. Relying on these annual cycles, the GCM seems to do a fairly good job in reproducing the low frequency changes of the buoy winds. The biggest signal is observed in early 1984 with strong northwesterly anomalies. The GCM simulates this feature nicely, but underestimates the zonal wind anomalies significantly.

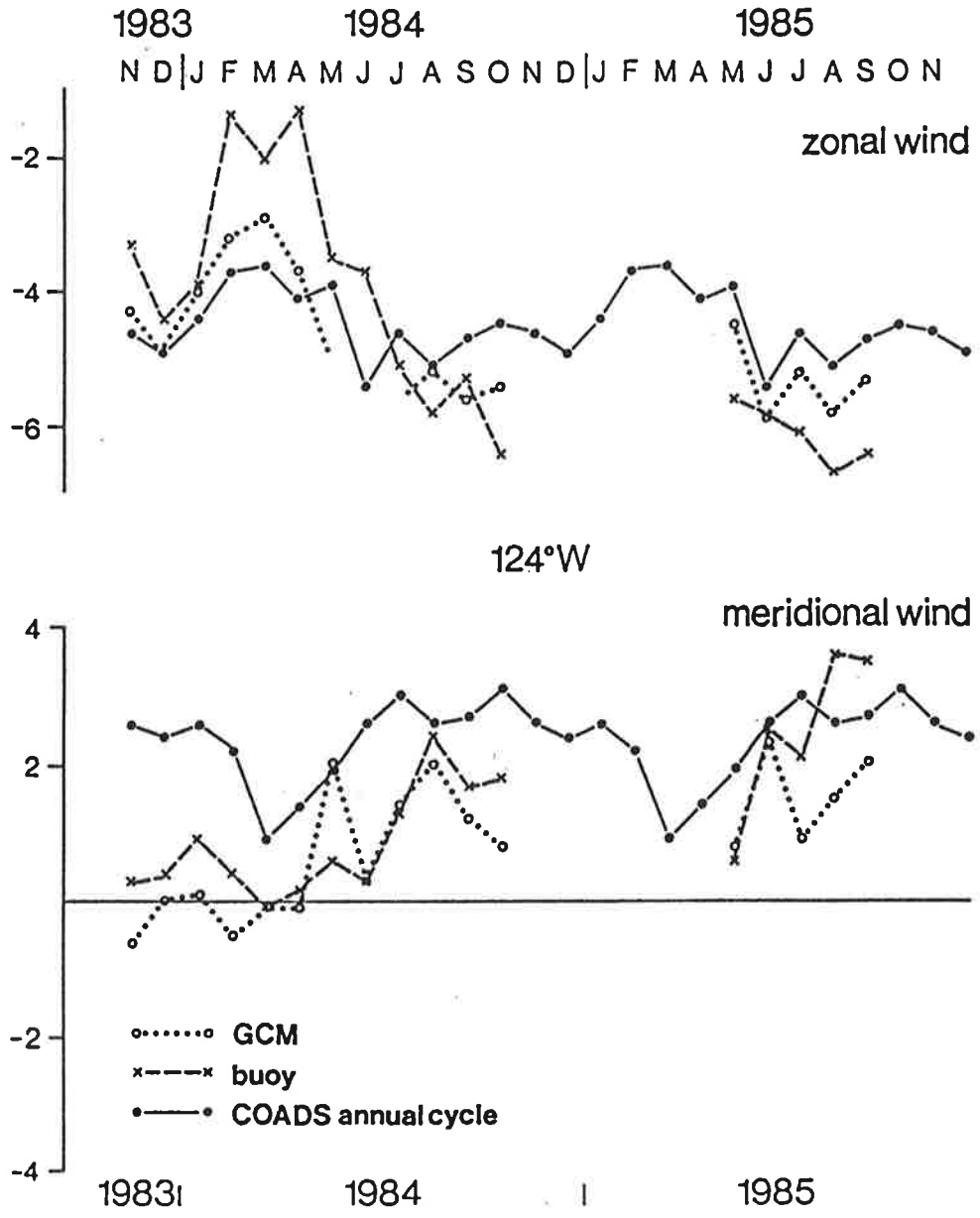

Figure 4: Time series of zonal (top) and meridional (bottom) 10 m wind at 124°W as reported from the buoy (crosses) and simulated in the GCM experiment (open circles). For comparison the mean annual cycle as derived from the 1950-79 COADS is added (filled circles). Units: m/s.

4. Results: Large Scale

4.1 The Southern Oscillation Index

As a measure of the state of the Southern Oscillation we use the classical SO index given by sea level pressure (SLP) difference between Darwin and Tahiti. The observed and simulated anomaly time series (Fig. 5) are not related to each other on time scales of a few months, but on time scales longer than a year the signs of the simulated and the observed SOIs coincide. Also, the observed warm events 1972/73 and 1982/83 are nicely reproduced by the model, and so is the cold phase of 1970/71. On the other hand, the model simulates the pair of cold events 1973/74 and 1975/76 and the period of fairly high SOI during 1976/77 only with significantly reduced strength.

The statistics of the two curves is summarized in the auto, coherence squared and phase spectra, shown in Figure 6. On time scales shorter than one year, the variances of both time series are similar, but the coherence is low (Fig. 6b). On time scales longer than two years, the GCM generated variance is clearly weaker than the observed variance (Fig. 6a). The coherence, however, is large (80% and more) and highly significant (risk < 1%) at these time scales and the phase spectrum (Fig. 6c) is close to zero. We conclude that the timing of simulated low frequency changes in the Southern Oscillation is adequately reproduced, but that the intensity of the modeled SO is too weak.

Carrying out the same analysis for the control run with climatological SST, no indication for a Southern Oscillation was found.

4.2 Tropospheric Winds and Precipitation: NMC Analyses

Figure 7 displays Hovmøller diagrams and distributions of variance of anomalous 850 mb zonal wind along the Pacific equator. The simulation (Fig. 7a) is compared to NMC analyses (data set C). The general pattern of positive and negative anomalies is quite similar but the variability of the observed field is much larger with respect to strength and spatial extent. This is substantiated by the curves showing the zonal distribution of variance in the GCM data and in the analyzed data: The GCM's variance is markedly confined to the western portion of the Tropical Pacific and in general much weaker than

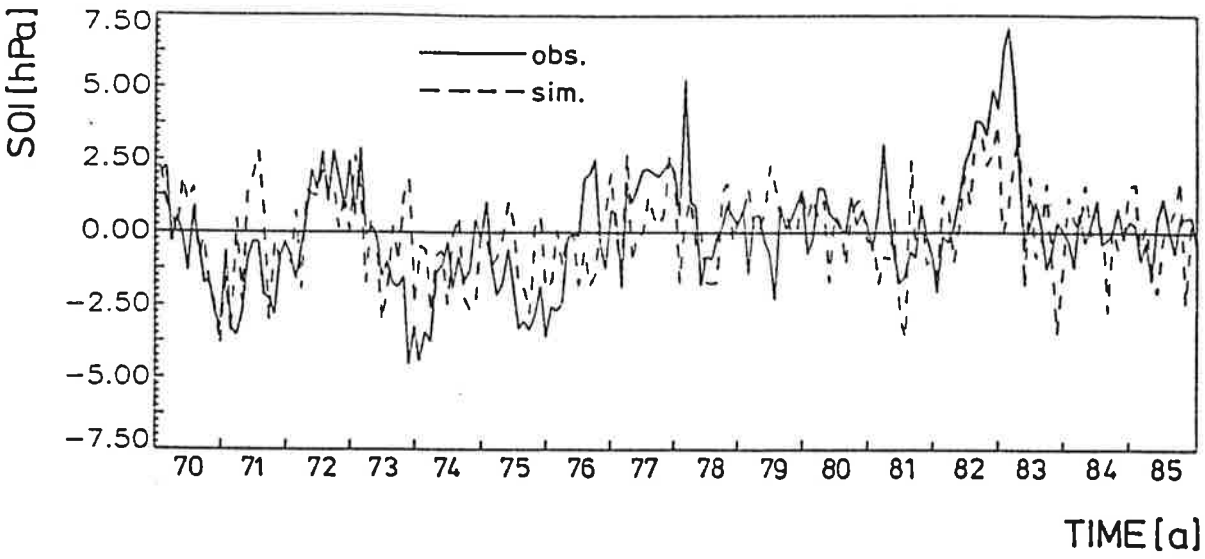

Figure 5: Simulated (dashed) and observed (solid) Southern Oscillation Index defined by the monthly mean difference of sea level pressure anomalies at Darwin and Tahiti

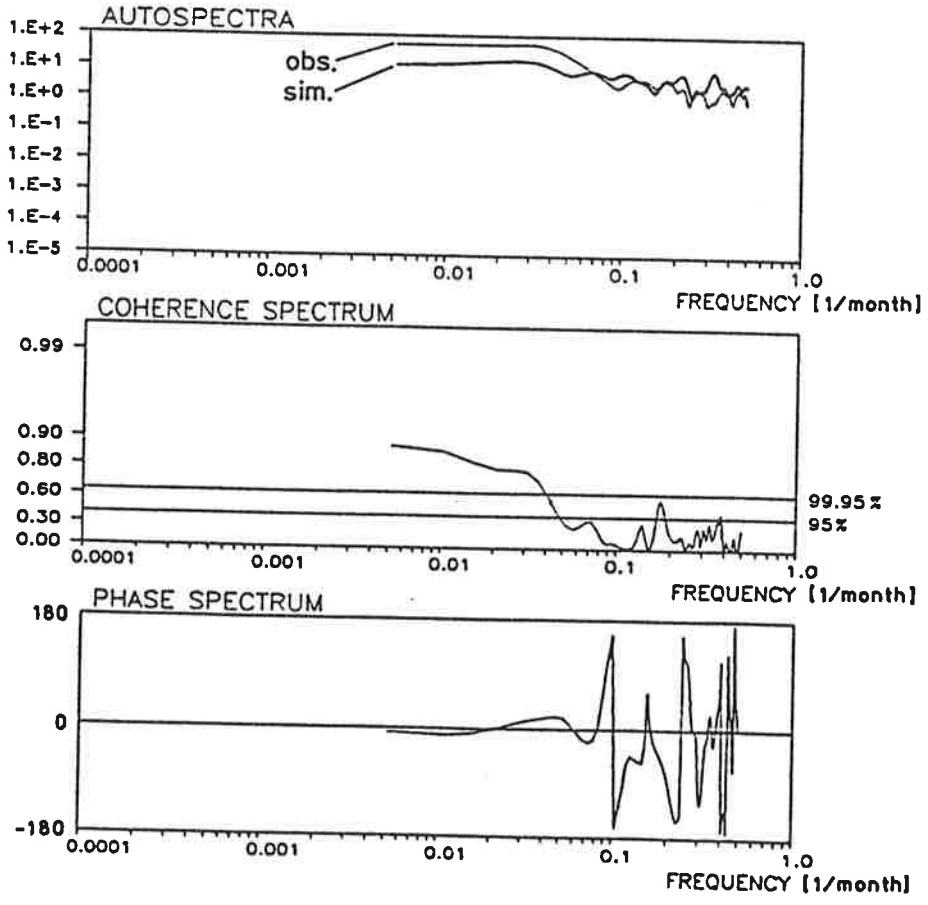

Figure 6: Autospectra (top), coherence squared (middle) and phase (bottom) spectrum of the simulated and observed Southern Oscillation Index shown in

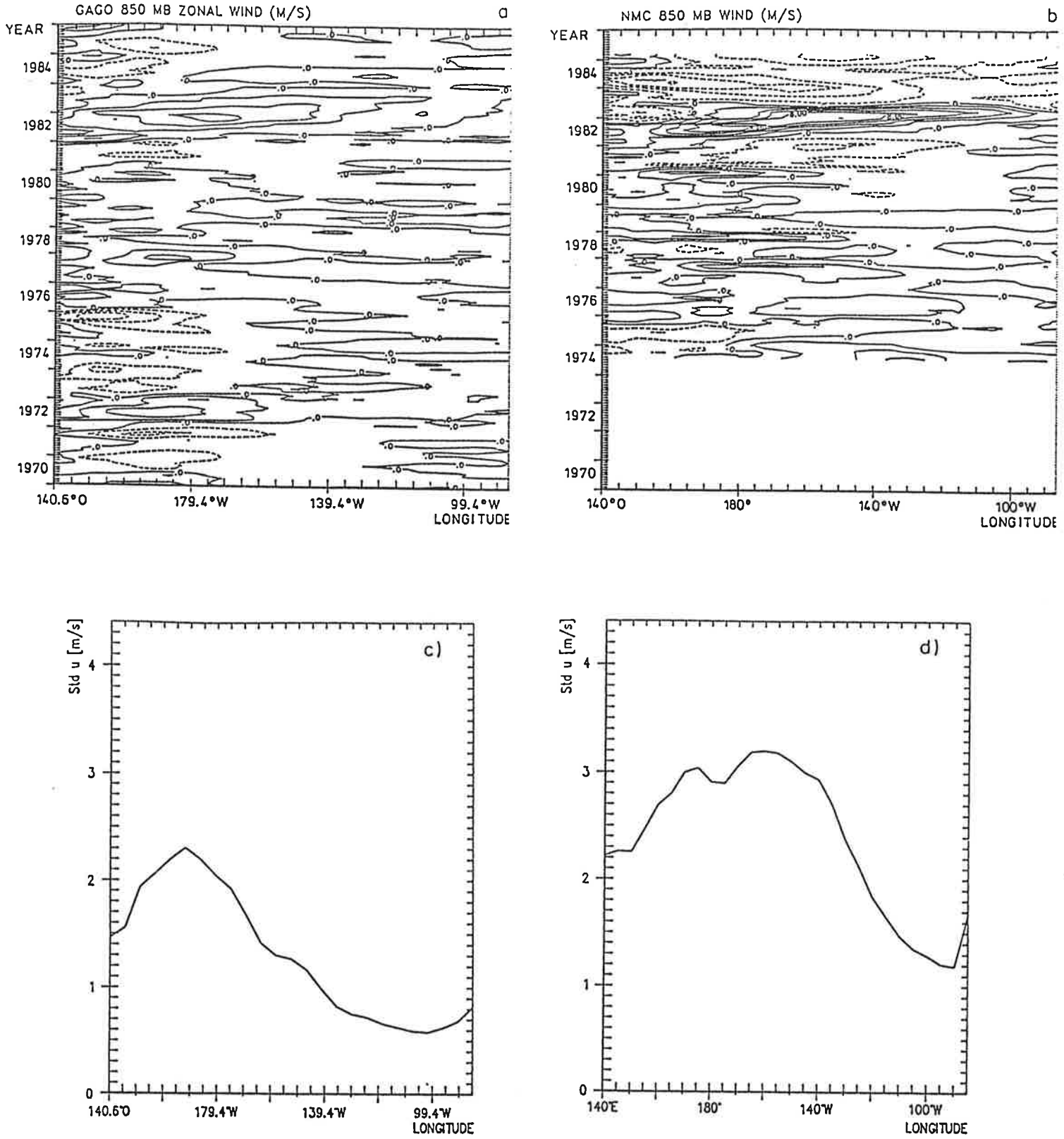

Figure 7: Hovmøller diagrams of 850 mb zonal wind along the equator (145°-85°W). Units: m/s. (a) GCM simulation: January 1970 to December 1985. (b) NMC analyses: January 1974 to mid 1984. (c) standard deviation (m/s) along the equator in the GCM simulation. (d) standard deviation (m/s) along the equator in the NMC analyses.

observed.

The most prominent feature in both, the NMC analyses and the GCM data, is the strong 1982/83 El Niño event: positive anomalies appear in early 1982 and travel across the basin with a speed of about 1 m/s. The above described deficiency of much too weak anomalies over the Eastern Pacific becomes very obvious as the event evolves. While in the beginning of the event zonal wind anomalies appearing over the Western Pacific are of comparable strength (maxima of 8 m/s and 10 m/s for the GCM and the NMC analyses, respectively) the GCM-generated anomalies become very weak as they propagate eastward. During spring of 1983, for instance, the GCM simulates anomalies of only 2 m/s at 120°W, which is much too weak compared to the observed 8 m/s. The easterly wind anomalies being characteristic for the time periods before and after that event, i.e. early 1981 to early 1982 and mid of 1983 until the end of 1983, with maximum wind anomalies of -6 m/s are not simulated.

Two more events are included in the NMC analyses, namely the strong cold event in 1975/76 (maximum -4 m/s) and the moderate warm event 1976/77 (4 m/s). The simulated wind anomalies of the former event are very strong (-8 m/s) but confined to the Western Pacific. The latter event is poorly simulated.

In Figure 8 Hovmøller diagrams of the anomalous three months running mean precipitation along the Pacific equator are presented. Also the zonal distributions of the simulated and the observed variances are displayed.

As for the tropospheric winds the signal associated with the 1982/83 El Niño is clearly identified in both data sets. In January 1982 positive anomalies of about 4 mm/month appear in the west, and, getting stronger, migrate eastward. In both diagrams maximum values of about 10 mm/month are reached in January/February 1983 at 150°W. At the same time anomalies have turned negative over the Western Pacific.

The general pattern of simulated and observed precipitation anomalies is quite similar, but other than for 850 mb winds the variance of the simulated values over the western part of the Pacific is of the same order of magnitude as observed. The variance over the Eastern Pacific, however, is again strongly underestimated.

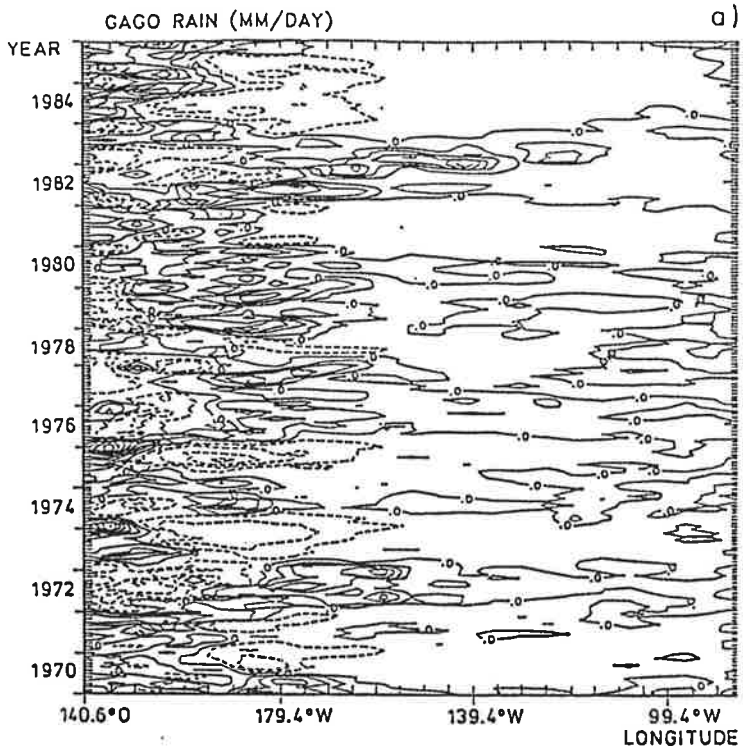

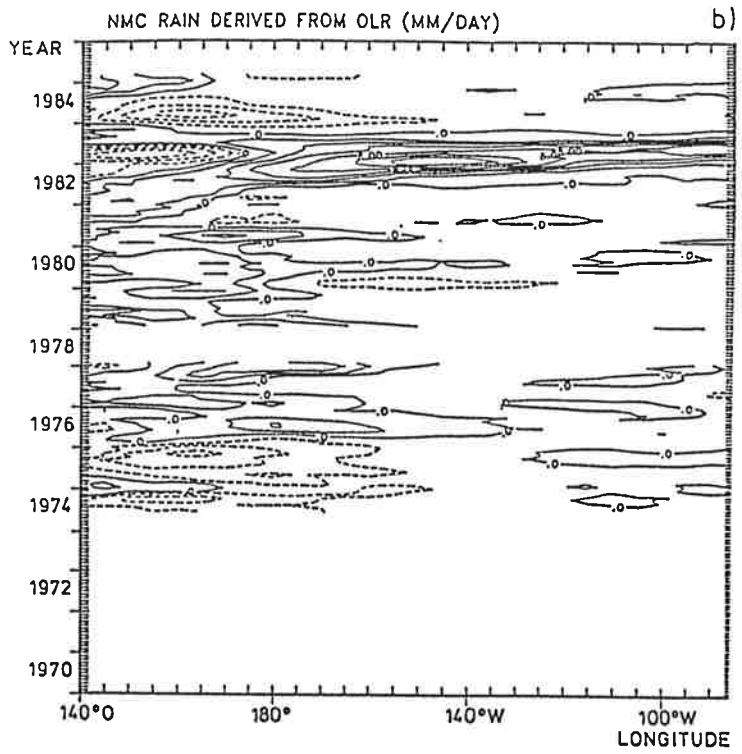

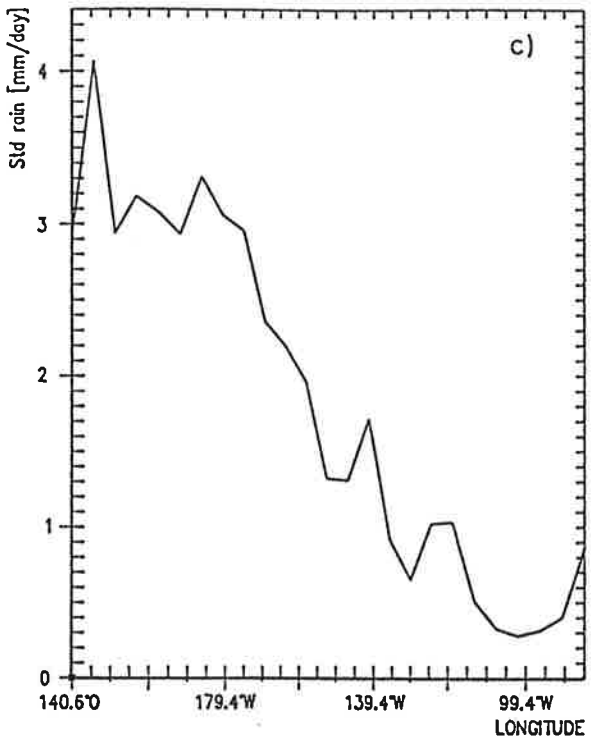

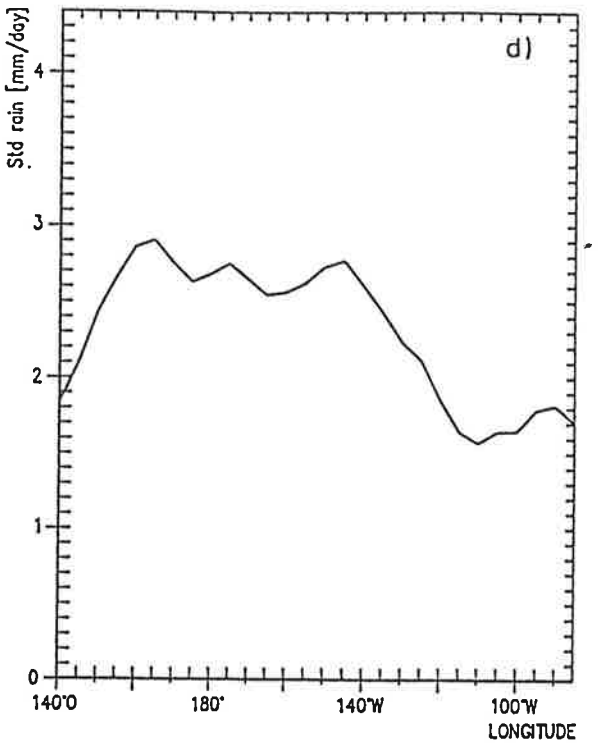

Figure 8: As Figure 7, but for rain fall. Units: mm/day. The NMC rain fall (b, d) has been obtained by deviding the OLR data by 5.7.

4.3 Surface Wind Stress

As verification data we use the FSU analyses of surface wind stress (data set D). We restrict ourselves to the zonal wind stress component, which is the most important forcing function for equatorial oceans. The annual cycle has been removed.

4.3.1 Local Comparison

We consider time series of zonal wind stress at 180° on the equator. Even if the data frequency at this position is poor, we selected this location because of its prominent role in air-sea interaction (Wyrtki, 1975). We considered also the data at 165°E, where observations are many. The results at this location are not shown, but were very similar to those at 180°. The time series of simulated and analyzed wind stress are given in Figure 9, the results of the cross spectral analysis in Figure 10.

Visual comparison of the two curves in Figure 9 reveals that the low frequency changes of zonal wind stress at this particular location are reasonably good reproduced by the GCM. The variance of the GCM-generated wind stress is clearly less than that of the analyzed data, a result which is substantiated by the autospectra showing the GCM variance being one order of magnitude smaller than the observed variance. The minimum at 0.08/month reflects the removal of the annual cycle. A statistical significant coherence squared is found for time scales between 20 and 50 months. The phase spectrum indicates that the observed time series leads the simulated by one or two months, but this lag is likely within sampling variability.

4.3.2 EOF Analysis

EOF analysis of low pass filtered (periods of less than 16 months have been removed) wind stress anomalies has been carried out for both the FSU data set and the GCM results. In both cases the first two EOFs, E_1 and E_2, of anomalous zonal wind stress explain more than half of the total variance (observation: 34% and 19%, simulation: 42% and 18%) whereas higher EOFs explain less than one tenth.

Both first (second) EOFs as well as their principal components are shown in

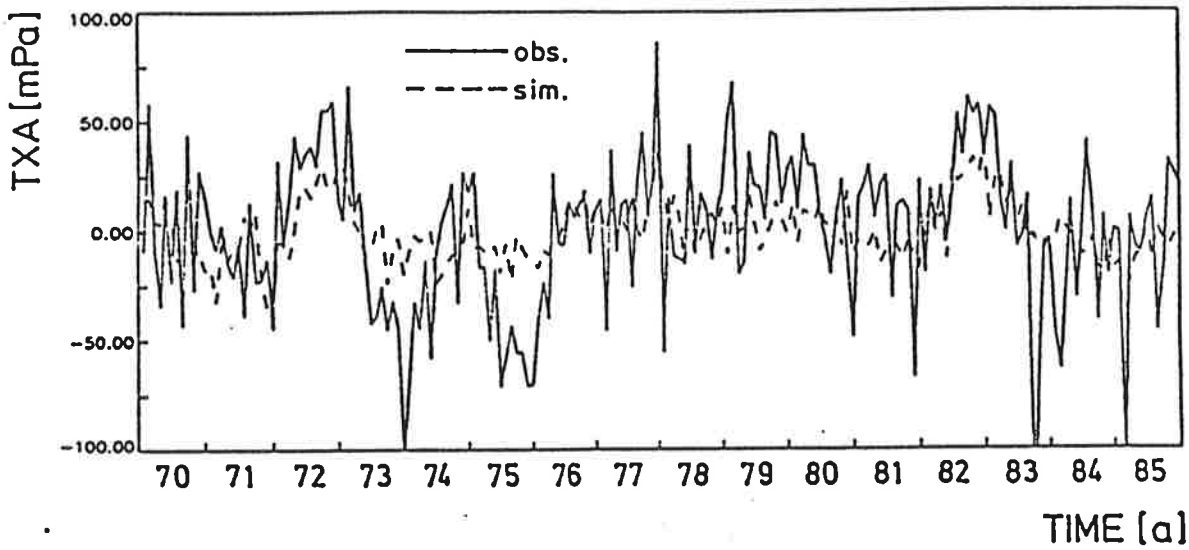

Figure 9: Time series of anomalous equatorial wind stress at 180° as extracted from the FSU wind stress analyses (solid line) and as simulated in the GCM experiment (dashed line). Units: mPa.

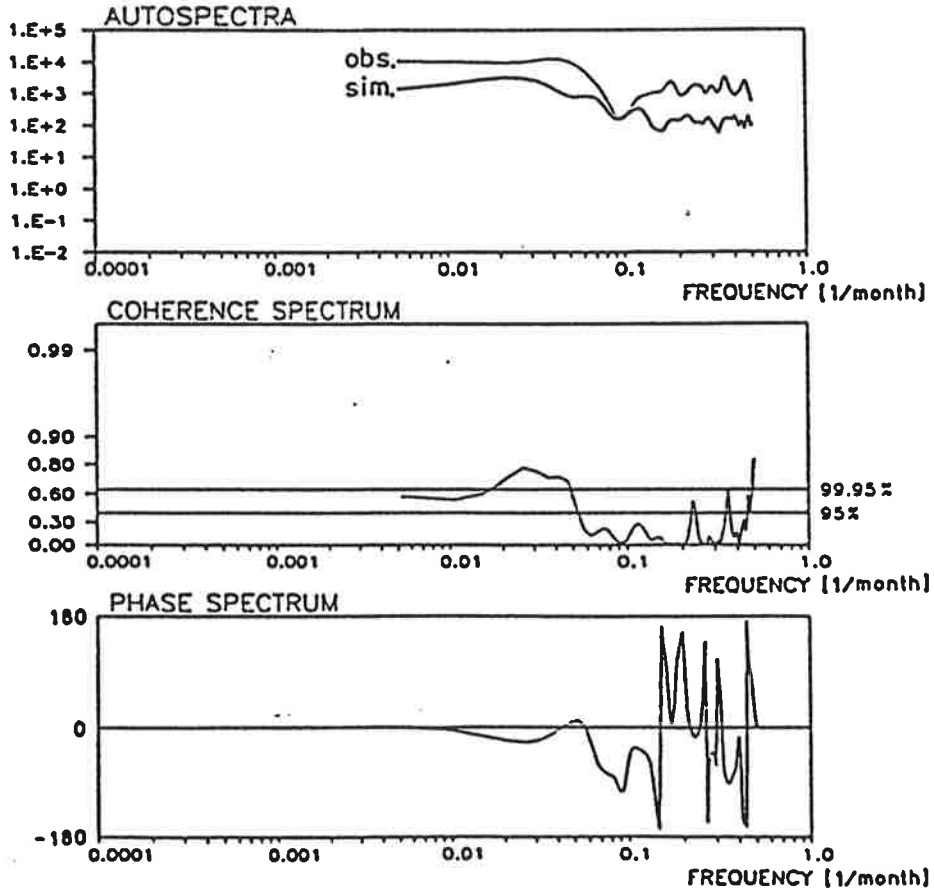

Figure 10: Cross spectral analysis of the time series shown in Figure 7. Top: autospectra; middle: coherence squared spectrum; bottom: phase spectrum.

Figure 11 (12). The spatial characteristics of E_1^{obs} and E_1^{GCM} are quite similar with large positive values over the Western Tropical Pacific with maximum on the equator near the dateline and smaller negative values east of 130°W. The observed tongue of positive values extending from the maximum to the south-east, reminding on the SPCZ, is not present in the simulation. The pattern of E_2^{obs} and E_2^{GCM} also show some similarities: In both patterns we find positive values on the equator extending from 150°E to the coast of South America, positive maxima at about 150°W, 10°S, and negative maxima north of Australia. This region of negative values, however, extends much more further to the east in the observations.

The corresponding first principal components (PC_1) are shown in Figure 11c. In the time series of the observed first principal component PC_1^{obs} all warm and cold phases of the Southern Oscillation can be easily identified, but in the simulated times series PC_1^{GCM} only the strong warm events of 1972/73 and 1982/83 as well as the moderate cold phase prior to 1972 are captured. Cross spectral analysis (not shown) reveals that the two time series have significant coherence squared for periods longer than 20 months.

As can be seen from Figure 12c the coefficient time series PC_1^{obs} and PC_2^{obs} of the first and second observed EOF vary over most of the 16 year period quite coherently with a phase shift of one half to one year. This may be interpreted as a "cyclic mode" with E_1^{obs} (Figure 11a) being the characteristic anomalies at the time of an El Niño (or a La Niña) event and E_2^{obs} (Figure 12a) describing an eastward shift during the transition phases between these events. An eastward propagation of zonal surface wind anomalies was also found by Barnett (1983) using the technique of complex EOFs, which is designed to extract progressive features within a multidimensional time series.

The cyclic behavior of the first two observed EOFs becomes very clear during the period of 1982/1983:

In March/April 1982 PC_2^{obs} has a minimum and, at the same time, PC_1^{obs} crosses the zero line. Thus the sum of the two contributions to the full signal reduces to $-E_2^{obs}$ with a large amplitude, i.e during the onset stage of the 1982/83 El Niño the observations show strong easterly wind stress anomalies between 5°N and 20°S and westerly anomalies south of 20°S and over most of the northern part of the basin.

At the end of 1982 when the event has fully developed with large SST anomalies in the Eastern Equatorial Pacific (not shown), the wind stress anomalies are dominated by E_1^{obs}, i.e., by large westerly anomalies over the Western and Central Equatorial Pacific.

In Spring 1983 we have to look at the pattern E_2^{obs} (E_1^{obs} is close to zero at this time): The westerly anomalies have moved to the east and are now centered at 150°W extending from Australia to the Peruvian coast.

At the end of 1983 again E_1^{obs} is dominant but with reversed sign: Over the eastern most part of the Pacific small westerly anomalies are left, but over the Western and Central Pacific wind stress anomalies now have a large easterly component.

Comparing the coefficient time series PC_1^{GCM} and PC_2^{GCM} derived from the GCM data, no coherent phase relationship appears (Figs. 11c and 12c), i.e., the first two simulated EOFs, E_1^{GCM} and E_2^{GCM}, do not describe a cyclic sequence of propagating patterns. There may be two reasons for this, namely: there is no pattern in the GCM data playing the role of E_2^{obs}, or this pattern is described by higher indexed EOFs or by a linear combination of EOFs. We will see later that the former reason is true.

5. Sensitivity of SST to Wind Stress Differences

The findings of the EOF analysis of simulated and observed zonal wind stress lead us to the following two hypotheses:

(I) That part of the observed wind stress variability, which is related to low frequency variations of SST can be described by the first two EOFs E_1^{obs} and E_2^{obs} only.

(II) The simulated wind stress field is insufficient to reproduce the complete observed sequence of El Niño and La Niña events, if it is used to drive an ocean model.

To assess the validity of these hypotheses the equatorial oceanic GCM, which is used in the coupled TOGA GCM (Latif et al., 1988a, 1988b), has been driven with various forcing fields for the period 1970 to 1985:

(a) The full observed wind stress forcing derived from FSU analyses,
(b) the observed forcing, which has been low-pass filtered and truncated to the first EOF shown in Figure 11a,
(c) the observed forcing, which has been low-pass filtered and truncated to the first two EOFs shown in Figures 11a and 12a,
(d) the full simulated wind stress forcing,
(e) the low pass filtered simulated forcing truncated to the first EOF shown in Figure 11b.

The experiments have been carried out by spinning up the ocean model with the observed (simulated) annual mean surface wind stress for one year and with the mean observed (simulated) annual cycle for four years. Thereafter the different anomalous forcing fields have been added to the mean annual cycle during the above described 16 years integrations.

The results obtained in experiment (a) have been presented in detail by Latif (1987), who compared the simulated SST with observed SST. He finds that low frequency variations of SST is favorably reproduced by the model in the Western Pacific. In the Eastern Pacific the results are less satisfying, but at least major El Niño episodes (1972/73 and 1982/83) are reproduced.

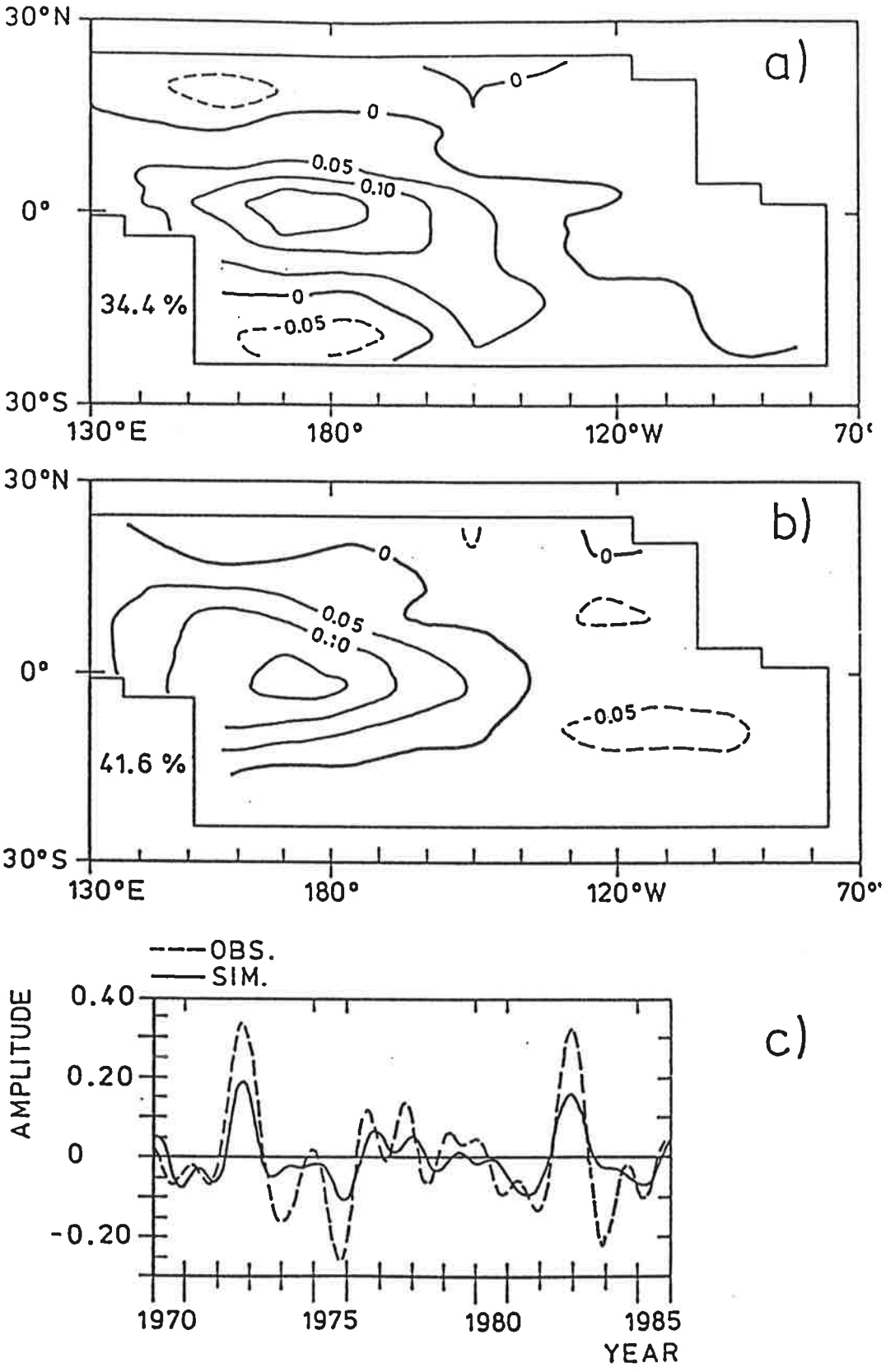

Figure 11: First Empirical Orthogonal Functions (EOFs) of low pass filtered (periods greater than 16 months are retained by filtering) zonal wind stress anomalies derived from 1961-85 FSU analyses (a) and from the GCM experiment (b). The explained variance is 34.4% for the observation and 41.6% for the simulation. The corresponding coefficient time series are shown in (c). Dashed line: FSU analyses. Solid line: GCM experiment

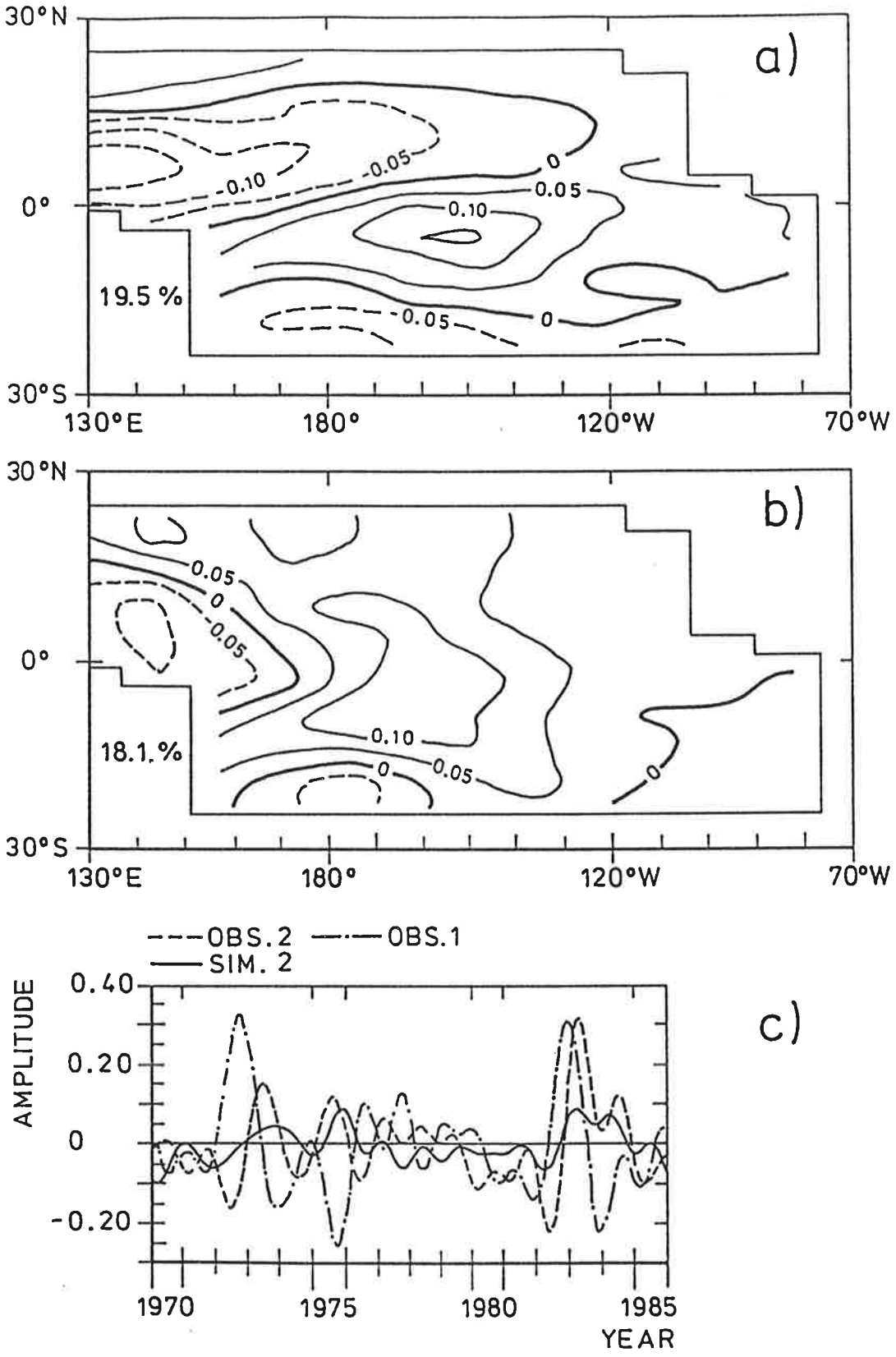

Figure 12: As Fig. 11 but for the second EOFs. Explained variances are 19.5% (observation) and 18.1% (simulation). For reference the coefficient time series of the first EOF derived from the FSU data set is added in (c).

In this and the following section we use the results of experiment (a) as a reference to compare the SST obtained in the other experiments with. The results are shown as time series of simulated SST anomalies at two equatorial locations: One at the dateline (Fig. 13) and the other in the Eastern Pacific at 110°W (Fig. 14). The SST simulated in (d) and (e) were almost identical. Therefore, SST simulated in (e) is not shown.

If we truncate the observed wind stress fields to the first EOF only (experiment (b)), the low frequency variability of SST at both considered locations is significantly weaker compared to the reference run (experiment (a)). At the dateline (Fig. 13a) this reduction is most pronounced during the major cold events of 1973, 1975, and 1983/84. The two major warm events of 1972/73 and 1982/83 are well simulated at this location. In the Eastern Pacific (Fig. 14a) low frequency variability is weak throughout the entire 16 years period. This result is a reflection of the spatial pattern of the first EOF (Fig. 11a), which has no significant contribution over the Eastern Pacific.

Adding the second EOF (experiment(c)) simulated SST anomalies at the dateline (Fig. 13a) become very close to the anomalies obtained in the reference run with full wind stress forcing. This is best seen for the three above mentioned major cold phases. The simulation of Eastern Pacific SST anomalies is also improved, if the second EOF is added. At this location, however, there still remain serious deviations to the reference run: First, a phase shift of a few months for the onset of the warm event of 1972/73, and second, a strongly reduced amplitude during the later stages of the 1982/83 warm event. Nevertheless, we conclude from the OGCM experiments (b) and (c) that most of the low frequency SST variability can be accounted for, if the first two EOFs are retained only in the wind stress field. Thus, we accept out hypothesis (I).

The SST anomalies obtained when the ocean model is forced with the full GCM simulated wind stress (experiment (d)) are shown in Figures 13b and 14b. As might have been guessed from the investigation of wind stress itself, the variance of SST is considerably reduced compared to the reference run. The ENSO signal in the Western Pacific is, apart from the two warm events of 1972/73 and 1982/83 much too weak. In the Eastern Pacific it is virtually absent, only the two afore mentioned warm events can be detected with severely underestimated amplitude. Thus, hypothesis (II) turns out to be correct also.

More important than the general underestimation of SST variance, however, is the similarity of the results obtained in the (d)-experiment with those obtained in the experiments (b) and (e), when only the first "observed" or "simulated" EOFs were used as anomalous forcing. From this similarity we infer that there is nothing in the simulated wind field which could play the role of the 2nd "observed" EOF, and that the ENSO-related SST signal in the "simulated forcing runs" is already obtained, if the ocean model is driven by the first "simulated" EOF only.

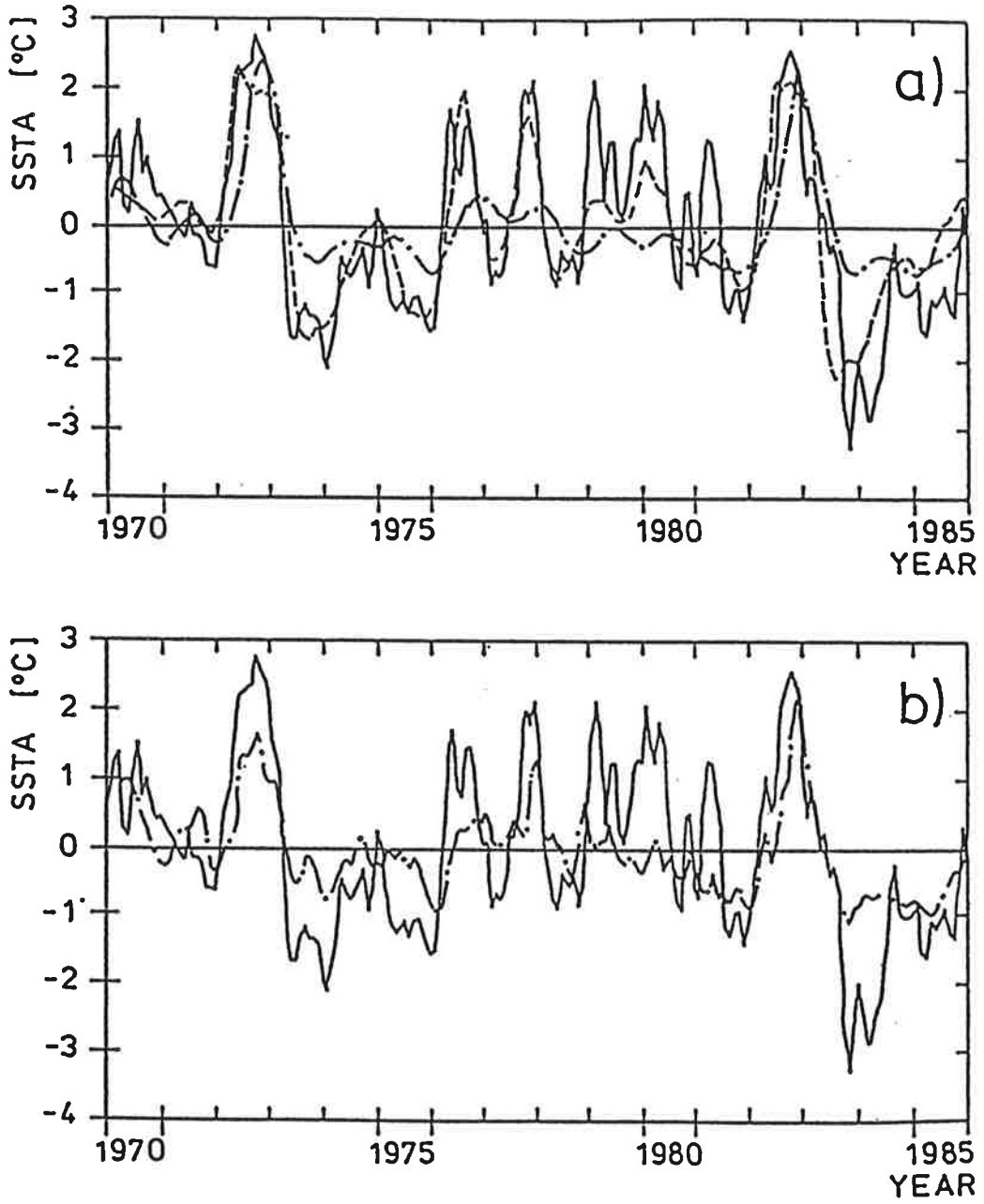

Figure 13: SST response of the OGCM on the equator at the dateline to (a) observed and (b) simulated wind stress. The solid lines show the SST anomalies which are obtained in the reference experiment (a) when the ocean model is forced with the FSU analyses. Dash-dotted lines: response to forcing which has been truncated to the first EOF (experiments (b) and (e)); dashed line: response to observed forcing truncated to the first two EOFs (experiment (c)).

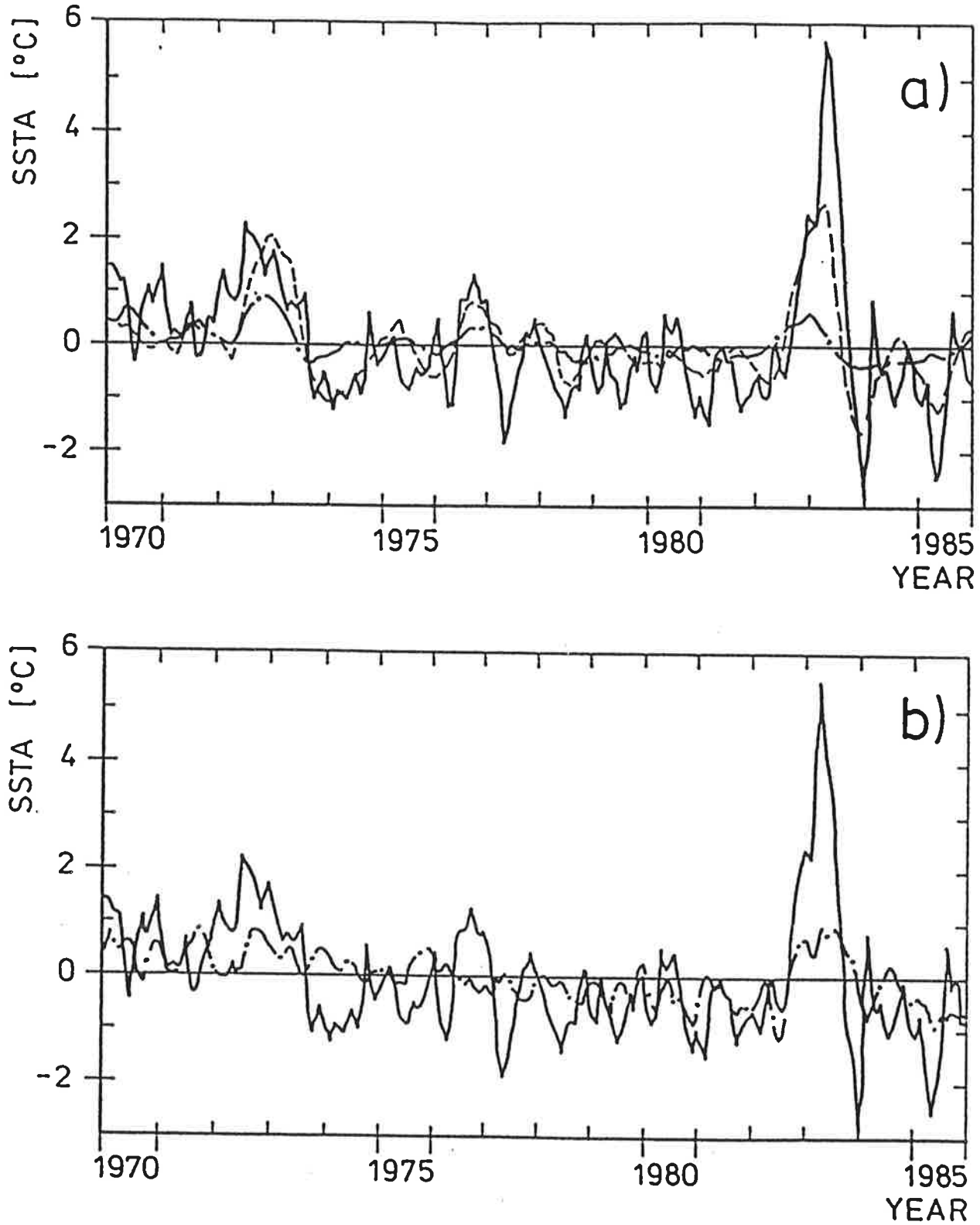

Figure 14: As Figure 13, but at 110°W.

6. Statistical A-Posteriori Improvement of Simulated Wind Stress

The results on the AGCM response found in the foregoing section are disappointing, because they indicate that the atmospheric GCM in its present form is not well suited to represent the atmospheric part of a coupled TOGA model. A possibility to overcome the shortcomings in simulated wind stress, at least for ENSO prediction studies with our coupled system, may be the application of Model Output Statics (MOS), a method which is routinely used in operational weather forecast (Glahn and Lowry, 1972). In this paper we use the technique as a diagnostic tool to find out, how the simulated wind stress anomalies may be changed to give a better ocean response.

If the observations at a certain time t are represented by a M-dimensional vector $\mathbf{q}(t)$ and the simulated data by a N-dimensional vector $\mathbf{p}(t)$, we are looking for a $M \times N$ matrix $\mathfrak{L}$ minimizing

$$\langle \| \mathfrak{L}\mathbf{p}(t) - \mathbf{q}(t) \|^2 \rangle \tag{1}$$

where $\| \cdot \|$ is the Euclidean vector norm and $\langle \cdot \rangle$ denotes expectation. $\mathfrak{L}$ is a linear operator that tells us how the simulated data p^1 to p^N must be changed to give on an average an optimal representation of the observations q^1 to q^M. Note that neither the number nor the physical parameter represented by the vectors $\mathbf{q}$ and $\mathbf{p}$ must be the same. For instance, $\mathbf{q}$ might represent 850 mb zonal wind on a fine grid and $\mathbf{p}$ surface wind stress on a coarse grid. The solution of (1) is given by

$$\mathfrak{L} = \langle \mathbf{q}(t)\mathbf{p}(t) \rangle \cdot \langle \mathbf{p}(t)\mathbf{p}(t) \rangle^{-1} \tag{2}$$

In our case, we use $\mathbf{q}$ = FSU analyses of zonal wind stress and $\mathbf{p}$ = GCM simulated wind stress, both interpolated onto the grid of the ocean model. We have different choices for designing the MOS approach:

(A) $\mathbf{q}$ and $\mathbf{p}$ represent the grid-point data covering the whole Tropical Pacific with $N = M = 650$,

(B) equation (1) is solved at each grid point separately, i.e. $N = M = 1$, with $\mathbf{q}$ and $\mathbf{p}$ observed and simulated wind stress at location j, respectively.

(C) $\mathbf{q}$ and $\mathbf{p}$ are composed of EOF coefficients PC_j^{obs} and PC_j^{GCM}.

Approach (A) is impracticable, because with the presently available data we can not derive a reliable estimate $\mathfrak{L}$ by means of (2), which requires the dimensions N and M to be significantly smaller than the number of available samples. In our case the latter number is 16 × 12 = 192 (number of years × 12 months). We call (2) LOS (Local Output Statistics) and (3) POS (Pattern Output Statistics).

After having determined the "correction matrix" $\mathfrak{L}$, the GCM generated wind stress anomalies can be corrected interactively in the coupled atmosphere-ocean system. In the present paper we investigate the possible merits of the MOS technique by forcing the ocean GCM with a-posteriori corrected wind stress, i.e., by $\mathfrak{L}\mathbf{p}$ instead by $\mathbf{p}$. The result of the correction are time series of zonal wind stress anomalies, whose statistics are determined from the observations, while their time evolution is computed by the AGCM.

The results of the LOS approach (2) and of the POS approach (3) are presented by showing the ocean GCM's response to the LOS and POS corrected GCM wind stress anomalies at the two equatorial locations already used in Section 5, namely 180° and 110°W (Fig. 15).

6.1 Results obtained with LOS

For the LOS approach (B) the matrix $\mathfrak{L}$ reduces to a single number estimated for each grid separately. In our case, $\mathfrak{L}$ varies between 1 and 2.5 over most portion of the Equatorial Pacific.

Using LOS-corrected GCM wind stress anomalies leads to a SST simulation which is very similar to that making use of POS corrected wind stress. Therefore, the LOS SST time series at the two equatorial locations are not shown. The reults are discussed together with the "POS-results" in the next section.

6.2 Results obtained with POS

For the POS approach (C) we use the two first principal components of low pass filtered wind stress, i.e., $N = M = 2$ and $\mathbf{q} = (PC_1^{obs}, PC_2^{obs})^T$ and $\mathbf{p} =$

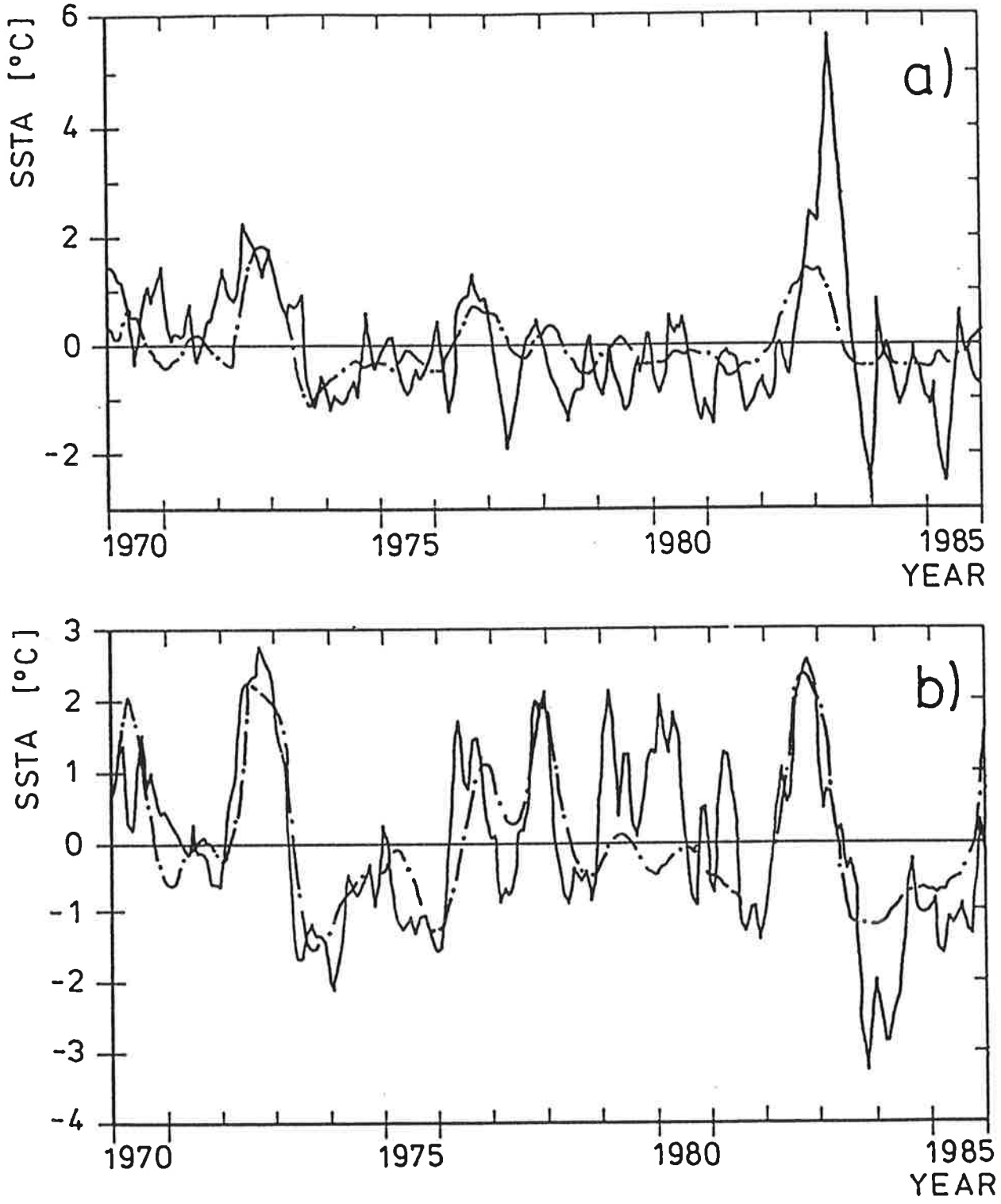

Figure 15: SST response of the OGCM on the equator at 110°W (a) and at the dateline (b) to POS-corrected simulated wind stress. The solid lines show the SST anomalies which are obtained in the reference experiment (a), when the ocean model is forced with the FSU analyses. Dash-dotted lines: response to POS-corrected wind stress.

$(PC_1^{GCM}, PC_2^{GCM})^T$. The correction matrix $\mathfrak{L}$ derived from (2) is

$$\mathfrak{L} = \begin{pmatrix} 1.71 & 0.53 \\ -0.23 & 1.40 \end{pmatrix}$$

This matrix describes an enhancement of the simulated principal components in the main diagonal (the elements are larger than 1) and a slight mixture of the two EOF coefficients.

The a-posteriori correction of wind stress anomalies for use in the ocean GCM is given by

$$\tau^* = \tau + \left[(E_1^{obs}, E_2^{obs}) \cdot \mathfrak{L} - (E_1^{GCM}, E_2^{GCM}) \right] \begin{pmatrix} PC_1^{GCM} \\ PC_2^{GCM} \end{pmatrix} \quad (3)$$

where τ denotes the "raw" GCM simulated and τ^* the corrected anomalous wind stress. Note that the POS approach (C) not only changes the variance but also the patterns by replacing the simulated EOF patterns by the observed EOF patterns.

POS and LOS both lead to an obvious improvement of the SST simulation on the ENSO time scale at the dateline (Fig. 15b), which is seen best for the two cold events of 1973 and 1975. Big deviations from the reference run are still found for the strong cooling following the 1982/83 event and the large positive anomalies during 1979 and 1980 in the Western Pacific. Interestingly, both of these features are not found in certain observations (see the Southern Oscillation Index, Fig. 5). So one might speculate (but by no means be certain) that by combining the information from the FSU analyses and the GCM output, and by restricting ourselves to the dominant parts, we can improve the forcing fields in some aspects. At the Eastern Equatorial Pacific location, LOS and POS lead to a moderate improvement (Fig. 15a). The big positive SST anomalies (up to almost 6 ^{o}C) during the 1982/83 El Niño cannot be simulated with that strength, because LOS and POS cannot account for extraordinary events, if the simulation is not extraordinary itself.

Using larger numbers for N and M did not improve our results significantly. On the other hand it is not sufficient to use the first EOF only, which can be deduced from hypothesis (I) presented in the preceding section.

7. Summary and Discussion

The tropical near surface response of the T21 model to globally varying observed 1970 to 1985 SST was compared to observational data. The comparison was more favorable for large scale data and for time periods longer than one year than it was for local data and shorter time scales.

Considering surface wind at selected equatorial locations, no similarities between simulated and observed data were found on the month to month time scale. To judge the agreement on the ENSO time scale the observed time series were too short (Figs. 2, 3, and 4).

The monthly mean SLP difference Tahiti minus Darwin clearly demonstrates that there is induced a Southern Oscillation in the model by the time dependent SST (Figs. 5 and 6), which is not present in a control run performed with climatologically varying SST. The model SO can also be identified in the other considered variables, i. e. low level wind, 850 mb wind, surface wind stress, and precipitation (Figs 7, 8, and 9).

The pattern and the phase of the simulated SO is correct, but the response is mainly restricted to the Western and Central Equatorial Pacific, which are key areas for the ocean-atmosphere interaction, whereas it is hardly detectable in the Eastern Equatorial Pacific.

The variance of the simulated low frequency variability is underestimated compared to the observations. An exception are the simulated rainfall anomalies which are, at least west of 150°W, of the same order of magnitude in both the simulations and the unfortunately rather short NMC time series (Fig. 8).

With respect to single events the model is fairly successful in reproducing the warm events in 1972/73 and 1982/83 and the cold event 1970/71. The cold events 1973/74 and 1975/76 and the moderate warm phases of 1976 and 1977 on the other hand can be identified in the simulations but are much less pronounced than observed.

An EOF-analysis of the observed zonal wind stress variability reveals that the Southern Oscillation may be described as an eastward migrating pattern centered on the equator. That is, the Southern Oscillation may formally be

written as a stochastic cyclic sequence of patterns,

$$\cdots \rightarrow E_1^{obs} \rightarrow E_2^{obs} \rightarrow -E_1^{obs} \rightarrow -E_2^{obs} \rightarrow E_1^{obs} \rightarrow E_2^{obs} \rightarrow \cdots$$

The characteristic numbers are: zonal length scale: 8000 km, meridional length scale: 4000 km; time scale: 2 years.

The simulated Southern Oscillation, on the other hand, may conveniently be described by just one EOF, as has been proven by the OGCM experiments. That is the simulated zonal wind stress anomalies have a dominant standing mode of low frequency variability and can therefore be described by the leading low frequency EOF only (Figs. 11 and 12).

$$\cdots \rightarrow E_1^{GCM} \rightarrow -E_1^{GCM} \rightarrow E_1^{GCM} \rightarrow -E_1^{GCM} \rightarrow \cdots$$

We conclude that the AGCM in its present version suffers from two major model flaws limiting its value to simulate tropical atmosphere-ocean interaction. First: While the patterns of the first zonal wind stress EOFs compare favorable with each other (Figs. 11a and 11b), the corresponding principal components (Fig. 11c) reveal a significant underestimation of the strength of the simulated anomalies. Second: The AGCM does not simulate the eastward migration of these anomalies, which could be inferred from the fact that the first two EOFs are not in quadrature to each other, as it is the case for the observations (Fig. 12). These deficiencies consequently lead to weak interannual variability which is particularly marked over the Eastern Pacific.

The underestimation of the strength of stress anomalies over the Western Pacific is probably closely related to the failure of the AGCM to simulate a realistic climate mean state, which is exemplified by much too weak Trades over the Pacific (Biercamp and Storch, 1987). Both errors might be related to the parameterization of deep convection, which presumably is not adequately tuned for our purposes, resulting in a weak sensitivity of the large scale tropical circulation to changes in SST.

It is not yet clear to us, why the AGCM fails to simulate the observed eastward migration of anomalies, since it is commonly accepted that at least for the 1982/83 El Niño the propagation of atmospheric anomalies was caused by the eastward migration of warm water across the Pacific (Gill and Rasmusson 1983). This was further supported by the model study of Fennessy and

Shukla (1988), who performed a realistic simulation of this particular event by prescribing observed SST. It is interesting that the AGCM developed at GFDL showed a similar result to ours. As described by Barnett (1985) the Southern Oscillation in this model appeared also as a standing feature. One possible reason why our AGCM failed may be the choice of the SST climatology (Alexander and Mobley, 1974), which exhibits systematically lower temperatures in the Eastern Pacific than other climatologies (e. g. Reynolds, 1988). For this reason temperatures of 29°C and more are hardly reached during the integration. The underestimation of tropical SST might limit deep convection in some areas and even inhibit at other locations. That is, the energy transfer might simply be cut off as the warm water moves eastward. Notice that the observations indicate the existence of 29°C-water in the Eastern Pacific in spring 1983 for several months (Gill and Rasmusson, 1983) and that in the model study of Fennessy and Shukla (1988) SST reached also similar values in the east.

Another major issue of this paper is to get more insight into the dynamics of our coupled ocean-atmosphere model (Latif et al. 1988a, b), which didn't show low frequency oscillations in a ten years integration. Our analysis of AGCM-simulated surface wind stress anomalies supports the speculation of Latif et al. 1988b that the weak interannual variability simulated by our coupled model may partly be attributed to the AGCM, which is unable to simulate wind stress anomalies of realistic strength so that the coupling may simply be too weak for oscillations to occur (certainly there are other problems in the coupled system, which can be attributed to the OGCM and the applied coupling technique).

Nevertheless, there might be a way out of this dilemma. Since the results of the AGCM simulation are highly coherent with observations, the application of the MOS-technique may help to overcome some of the problems. We have shown that the simulation of SST anomalies can be significantly improved, if MOS-corrected wind stress anomalies are used as anomalous forcing (Fig. 15). This multiplicative correction scheme is presently being tested in ENSO hindcast experiments with our coupled model. Such a correction, however, could only be an intermediate solution until our AGCM has been improved to give a more realistic response to anomalous SST.

7. ACKNOWLEDGEMENTS

We thank Phil Arkin for the NMC data, Peter B. Wright for the Southern Oscillation Index and Marion Grunert, who thoroughly prepared the diagrams. We also wish to express our gratitude to the Director of the Max Planck Institut für Meteorologie, Klaus Hasselmann, for continously encouraging and supporting us. The work was in part financed by the European Community / Natural Hazards program under grant EV4C - 0035 - D(B).

REFERENCES

Alexander, R. C. and R. L. Mobley, 1974: Monthly average sea surface temperature and ice pack limits for 1 deg global grid. RAND Rep., R-1310-ARPA, 30 pp.

Arkin, P.A., 1982: The relationship between interannual variability in the 200 hPa tropical wind field and the Southern Oscillation.-Mon. Wea. Rev. 110, 1393-1404.

Barnett, T.P., 1983: Interaction of the monsoon and the Pacific Trade wind system at interannual time scales. Part I: The equatorial zone. Mon. Wea. Rev. 111(4), 756-773.

Barnett, T.P., 1985: Variations in near-global sea level pressure. J. Atmos. Sci., Vol. 42, No. 5, 478-501.

Biercamp, J., H. v. Storch, 1987: Exchange of energy and momentum at the ocean's surface. - "Climate simulations with the ECMWF T21 model in Hamburg.", Large Scale Atmospheric Modelling Report 1, 1986, Ed: G. Fischer (Meteorologisches Institut der Universität Hamburg, Bundessstr. 55, D2000 Hamburg 13, FR Germany), 83-94.

Chervin, R.M., 1986: On the impact of interannually varying ocean surface temperatures on the variability of southern hemisphere time-averaged atmospheric states. - preprint Volume Second International Conference on Southern Hemisphere Meteorology Dec 1-5, 1986, Wellington., 208-211.

Dümenil, L., U. Schlese, 1987: Description of the General Circulation model. - "Climate simulations with the ECMWF T21 model in Hamburg.", Large Scale Atmospheric Modelling Report 1, Ed: G. Fischer (Meteorologisches Institut der Universität Hamburg, Bundessstr. 55, 2000 Hamburg 13, FR Germany), 3-10.

Fennessy, M. J. and J. Shukla, 1988: Numerical simulation of the atmospheric response to the time-varying El Niño SST anomalies during May 1982 through October 1983. J. Climate, Vol 1, No 2, 195-211.

Fischer, G., 1987: "Climate simulations with the ECMWF T21 model in Hamburg.", Large Scale Atmospheric Modelling Report 1, Ed: G. Fischer (Meteorologisches Institut der Universität Hamburg, Bundessstr. 55, 2000 Hamburg 13, FR Germany), 3-10.

Freitag, H.P., M. J. McPhaden, A.J. Shepherd, 1988: Comparison of equatorial winds as measured by cup vs. propeller anemometers. - Contribution No. 1023 from NOAA / Pacific Marine Environmental Laboratory.

Gill, A. E. and E. M. Rasmusson, 1983: The 1982-83 climate anomaly in the equatorial Pacific. Nature 306(5940), 229-234.

Glahn, H.R., and D.A. Lowry, 1972: The use of model output statistics (MOS) in weather forecasting. - J. Appl. Meteor. 11, 1203-1211.

Goldenberg, S.B., J.J. O'Brien, 1981: Time and space variability of tropical Pacific wind stress. - Mon. Wea. Rev. 109, 1190-1207.

Graham, N.E., T.P. Barnett, R.M. Chervin, M.E. Schlesinger, U. Schlese, 1988: Comparisons of GCM and observed surface wind fields over the tropical indian and pacific oceans. In preparation for J. Atmos. Sci..

Han, Y.J., S.W. Lee, 1981: A new analysis of monthly mean wind stress over the global ocean. - Climate Research Institute Report 26, Oregon State University, Corvallis, Oregon.

Kiladis, G., 1988: Some comments on the T 21 model's precipitation climatology. "Climate simulations with the ECMWF T21 model in Hamburg.", Large Scale Atmospheric Modelling Report 4, Ed: H. von Storch (Meteorologisches Institut der Universität Hamburg, Bundessstr. 55, 2000 Hamburg 13, FR Germany), 3-10.

Kirk, E., M. Ponater, A. Kirk, 1987: Circulation statistics of the T21 GCM. - "Climate simulations with the ECMWF T21 model in Hamburg.", Large Scale Atmospheric Modelling Report 1, 1986, Ed: G. Fischer (Meteorologisches Institut der Universität Hamburg, Bundessstr. 55, 2000 Hamburg 13, FR Germany), 11-30.

Large, W.G., S. Pond, 1981: Open ocean momentum flux measurements in moderate to strong winds. - J. Phys. Oceano. 11, 324-336.

Latif, M., 1987: Tropical ocean circulation experiments. - J. Phys. Oceano. 17, 246-263.

Latif, M., J. Biercamp, and H. von Storch, 1988a: The response of a coupled ocean-atmosphere general circulation model to wind bursts. - J. Atmos. Sci. 45, 964-979.

Latif, M., J. Biercamp, H.v. Storch, F.J. Zwiers, 1988b: A ten year climate simulation with a coupled ocean-atmosphere general circulation model. in preparation.

Lau, N.-C., 1985: Modeling the seasonal dependence of the atmospheric response to observed El Ninos in 1962-76. - Mon. Wea. Rev. 113, 1970-1996.

Leetmaa, A., M. Ji, 1988: Operational hindcasting of the tropical pacific. Submitted to Dyn. of Atm. a. Oc.

Legler, D.M., J.J. O'Brien, 1984: Atlas of tropical Pacific wind stress climatology 1971-1980. - Florida State University, Department of Meteorology, Tallahassee FL 32306.

McPhaden, M., B.A. Taft, 1988: On the dynamics of seasonal and intraseasonal variability in the eastern equatorial Pacific. - submitted to J. Phys. Oceanogr. (Contribution No. 960 from NOAA/PMEL).

Reynolds, R. W.., 1988: A real-time global sea surface temperature analysis. J. Climate, Vol 1, No.1.

Storch, H. v., 1988: "Climate simulations with the ECMWF T21 model in Hamburg.", Large Scale Atmospheric Modelling Report 4, Ed: H. von Storch (Meteorologisches Institut der Universität Hamburg, Bundessstr. 55, 2000 Hamburg 13, FR Germany), 3-10.

Trenberth, K.E., J. G. Olson, 1988: Evaluation of NMC global analyses: 1979-1987. - NCAR Technical Note NCAR/TN-299+STR.

Wallace, J. M., Q. Jiang, 1987: On the observed structure of the interannual variability of the atmosphere/ocean climate system. - Atmospheric and Oceanic Variability (H. Cattle, editor), Royal Met. Soc.

Wright, P.B., 1988: At atlas based on the 'COADS' data set: Fields of mean wind, cloudiness and humidity at the surface of the global ocean. - MPI report14 (Max Planck Institut fuer Meteorologie, Bundesstrasse 55, 2000 Hamburg 13, FR Germany).

Wyrtki, K., 1975: El Nino - dynamical response of the equatorial Pacific ocean to atmospheric forcing. - J. Phys. Oceanogr. 5, 572-584.